HMG Advance Access published August 4, 2009



# A conserved role for the mitochondrial citrate transporter Sea/SLC25A1 in the maintenance of chromosome integrity

Patrizia Morciano[1,8¶], Chiara Carrisi[2¶], Loredana Capobianco[2], Linda Mannini[3], Giosalba Burgio[4], Gianluca Cestra[5], Giuseppe E. De Benedetto[6], Davide F.V Corona[4], Antonio Musio[3,7], Giovanni Cenci[1*]

[1]Dipartimento di Biologia di Base ed Applicata, Università dell'Aquila, 67010 L'Aquila, Italy; [2]Dipartimento di Scienze e Tecnologie Biologiche ed Ambientali, Università del Salento, 73100 Lecce, Italy; [3]Istituto di Tecnologie Biomediche, CNR, 56124 Pisa, Italy; [4]Dipartimento di Biologia Cellulare e dello Sviluppo and Istituto Telethon Dulbecco, Universita' degli Studi di Palermo, 90127 Palermo, Italy; [5]Dipartimento di Genetica e Biologia Molecolare, Università La Sapienza, 00185 Roma, Italy; [6]Dipartimento dei Beni Artistici e Storici, Università del Salento, 73100 Lecce, Italy; [7]Istituto Toscano Tumori, 50139 Firenze, Italy; [8]Present address: LBMB, NCI, NIH, Bethesda, MD 20892

¶These authors contributed equally to this work

* Corresponding Author

Giovanni Cenci, PhD
Dip.to Biologia di Base ed Applicata
Università dell'Aquila
Via Vetoio, Loc. Coppito
67010 Coppito, L'Aquila (IT)
giovanni.cenci@cc.univaq.it
tel 39 0862 433299 office
39 0862 433553 lab
fax 39 0862 433273

## Abstract

Histone acetylation plays essential roles in cell cycle progression, DNA repair, gene expression, and silencing. Although the knowledge regarding the roles of acetylation of histone lysine residues is rapidly growing, very little is known about the biochemical pathways providing the nucleus with metabolites necessary for physiological chromatin acetylation. Here we show that mutations in the *scheggia (sea)*-encoded Sea protein, the *Drosophila* ortholog of the human mitochondrial citrate carrier *SLC25A1*, impair citrate transport from mitochondria to the cytosol. Interestingly, inhibition of *sea* expression results in extensive chromosome breakage in mitotic cells and induces an ATR-dependent cell cycle arrest associated with a dramatic reduction of global histone acetylation. Notably, loss of *SLC25A1* in siRNA-treated human primary fibroblasts also leads to chromosome breaks and histone acetylation defects, suggesting an evolutionary conserved role for Sea/SLC25A1 in the regulation of chromosome integrity. This study therefore provides an intriguing and unexpected link between intermediary metabolism and epigenetic control of genome stability**.**

## Introduction

The maintenance of genome integrity represents an immense challenge for all eukaryotic cells, which are continuously exposed to environmental and metabolic insults that damage DNA. The accuracy with which cells replicate their genomes results from the coordination between constant monitoring of DNA integrity and efficient repairing of damaged DNA (1). In higher eukaryotes, a failure to repair DNA damage can lead to high frequencies of mutations, genetic disease and cancer development (2-4). One of the most hazardous type of DNA damage is a double-strand break (DSB), which can be generated by genotoxic agents or be self-inflicted by the cell (5, 6). DSBs are repaired by various mechanisms (7) that require modifications of chromatin to work efficiently (8, 9). These changes in chromatin structures occur mostly as a result of histone covalent modifications that function in concert with nucleosome remodelling enzymes (9-11). In particular, histone acetylation has emerged as a major post-translation modification which, along with transcription modulation, plays an important role in other biological processes, such as replication and DNA repair (12, 13). Although our knowledge of the acetylation of histone lysine residues is rapidly improving, the identification of biochemical pathways providing the metabolites necessary for physiological chromatin acetylation is still pending.

We report that mutations in the *Drosophila* mitochondrial citrate transporter gene *scheggia (sea)* and in its human ortholog SLC25A1 affect the efflux of citrate from mitochondria to cytosol, cause a global reduction of histone acetylation, and lead to extensive chromosomal breakage. Our findings indicate that Sea/SLC25A1 is required to prevent chromosome breaks, highlighting a conserved and unprecedented link between citrate metabolism, chromatin acetylation and chromosome integrity.

## Results

### *scheggia (sea)* is required for chromosome integrity in Drosophila

As part of a screen for mutations affecting chromosomal integrity, we found that *Drosophila* mutant brain cells, either homozygous or hemizygous for the P-element induced late lethal mutation *l(3)EP3364,* exhibit frequent (~40%) chromatid and chromosome breaks, as well as chromosome exchanges (~3%) (Figure 1). This suggests that such a mutation specifies a gene required to prevent chromosome breakage in both $G_1$ and S-$G_2$. In addition, ~10% of mutant cells exhibited a more complex breakage phenotype consisting of multiple chromosome splinters (Figure 1F). The gene specified by this mutation was named *scheggia (sea)* after its chromosome splinter ("scheggia" in Italian) phenotype and the *l(3)EP3364* genetically null allele (Figure 1G) is henceforth indicated as $sea^{EP}$. *sea* mutant neuroblasts showed a ~3-fold reduction of the mitotic index (MI) with respect to wild type, while the frequency of anaphases (AF) were indistinguishable from wild type (Figure 1H). This indicates a cell cycle delay before the M-phase. To investigate whether the delay was due to the activation of the DNA Damage Response (DDR), we generated double mutants for *sea* and genes involved in this process: *mei-41,* encoding the fly homolog of ATR (14); *mus304,* which encodes the ATR-interacting protein ATRIP (15); and *rad50* and *mre11,* whose products are part of the Mre11/Rad50/Nbs complex (16). We found that *mei-41* and *mus304,* but not the *rad50* and *mre11* mutations override the cell cycle block induced by *sea,* causing a ~2.5-fold increase of the MI relative to that observed in *sea* single mutant (Figure 1H). We also generated *sea* and *telomere fusion (tefu)* (encoding the fly homolog of ATM (17-19) double mutants. However, these larvae died early during the development, preventing an assessment of the role of Tefu/Atm in the *sea*-induced block (data not shown). Thus, the interphase arrest in *sea* mutants occurs independently of the MRN complex and is mediated by a signaling pathway involving at least ATR and ATRIP.

By sequencing the genomic region adjacent to the $sea^{EP}$ insertion, we found that the insertion site is 437 nucleotides upstream from the putative ATG of *CG6782*. This position differs from that indicated in Flybase that places the P-element insertion 955 nucleotides from the start codon (Figure S1). The $sea^{EP}$ specific phenotypes are rescued by a wild-type *CG6782* transgene, confirming that they are indeed due to the insertion in this gene. Therefore, *CG6782* will be henceforth referred to as *scheggia (sea)* and its product as Sea.

Semi quantitative (sq)RT-PCR revealed a 60-70% reduction of *sea* transcript levels in $sea^{EP}$ (Figure S1). We generated new late-lethal alleles by P-element excision. Most of them (e.g. $sea^{\Delta 24}$) are deletions of the original P-element that still severely affected transcription levels of *sea* (Figure S1). In addition, chromosome break frequencies as well as MI defects observed in these new alleles are indistinguishable from that of $sea^{EP}$ (Figure 1G and 1H), indicating that these additional alleles are severely hypomorphic.

**Functional characterization of Sea, the ortholog of the tricarboxylate carrier SLC25A1**

*sea* encodes the ortholog of the mammalian mitochondrial citrate transporter SLC25A1, also known as the tricarboxylate carrier (Figure S2)(20, 21). SLC25A1 is a transport protein of the inner mitochondrial membrane that exports citrate from the mitochondria to the cytosol, where it is cleaved by ATP-citrate lyase to oxaloacetate and acetyl CoA units necessary for de novo fatty acid and sterol biosynthesis (20)(Figure S8). Interestingly, the biochemical characterization of the *Drosophila* Sea protein indicates that this carrier shows transport properties similar to those of other citrate mitochondrial carriers (including mammalian SLC25A1) (21).

We generated and affinity-purified an anti-Sea polyclonal antibody that specifically recognizes a protein of the expected molecular weight (~ 33 KDa) in blotted mitochondrial lysates (Figure 2A). Sea levels are ~60% reduced in *sea* mutants compared to wild-type in agreement with our sqRT-PCR data (Figure 2A). Anti-Sea immunostaining showed a punctuate localization of Sea

exclusively in the larval neuroblast cytosol that co-localizes with Skap, a resident protein of the inner mitochondrial membrane (22), indicating that anti-Sea decorates mitochondria (Figure 2B and 2E). As expected, Sea localization is strongly reduced in *sea* mutants (Figure 2C), confirming our Western blot data. Sea also co-localizes with the nebenkern, a mitochondrial formation in *Drosophila* spermatids that results from the aggregation of mitochondria just after male meiosis is completed (Figure S3).

Time course of citrate uptake for Sea was measured in proteolisosomes reconstituted with mitochondrial extracts. This assay revealed a ~70% reduction of [$^{14}$C]citrate/citrate exchange in *sea* mutants with respect to wild-type (Figure 2F). Moreover, while the Km of citrate transport activity in *sea* mutants did not significantly change compared to wild type (0.133± 0.04 μM vs 0.132±0.023 μM), the Vmax value was strongly reduced in *sea* mutant (86.3±1.087 nmol/min X mg protein) with respect to wild-type (331.498± 0.995 nmol/min X mg protein). This indicates that reduction of Sea affects citrate transport but not the affinity of transporter for the substrate. Furthermore, Gas Chromatography/Mass Spectrometry (GC/MS) analysis revealed a ~70% decrease of cytosolic (but not mitochondrial) citrate levels in the mutants compared to wild type (Figure 2G), strongly suggesting that a reduction of Sea influences the overall levels of citrate in the cytosol. In addition, we found that *sea* mutants exhibited normal citrate synthase activity (an indicator of mitochondria integrity) and no increase of reactive oxygen species (ROS) (Figure S7 and Supporting Information), indicating that the *sea*-induced cell cycle delay is not determined by a mitochondrial retrograde response which is activated upon mitochondrial dysfunction (23). Together, our data show unambiguously that Sea is a *Drosophila* mitochondrial protein that transports the citrate from the mitochondria to the cytoplasm.

To better link the *sea*-chromosome breakage phenotype to deprivation of cytosolic citrate, we investigated whether supplementation of *sea* mutant larvae with citrate could rescue chromosome abnormalities. Neuroblasts from *sea* mutant larvae fed with 0.1 M citrate show a statistically

significant reduction in the frequency of chromosome breaks (Figure 2H), suggesting that normal levels of citrate in the cell are required for chromosome integrity.

**Sea dysfunction affects histone acetylation.**

To address the role of Sea in chromosome stability, we wanted to investigate whether the reduction of the cytosolic citrate pool, and concomitantly of Acetyl CoA, affects the acetylation of some chromatin components. We immunostained *sea* mutant polytene chromosomes with an anti-Acetyl Lysine (Ac-Lys) antibody that recognizes multiple acetylated proteins including acetylated histones. 80% (n=60) of *sea* polytene chromosomes showed a strong reduction of Ac-Lys pattern compared to wild-type Oregon/R chromosomes (5% ; n=50) (Figure 3A). In addition, Western blots of mutant chromosome protein extracts probed with the same anti-Ac Lys antibody showed reduced levels of low-molecular-weight acetylated proteins, in relation to wild type extracts (Figure 3B). By stripping and reprobing the blot with anti-histone antibodies, we found that the low-molecular-weight bands correspond to histones (data not shown) confirming that acetylation of histones is specifically linked to the pool of citrate-derived acetyl-CoA (24). To better define the degree of histone acetylation in *sea* mutants, we immunostained *sea* mutant polytene chromosomes with anti-pan acetylated H2A, H2B, H3 and H4 antibodies. ~70% of polytene (n=50 for each immunostaining) mutant nuclei exhibited a strong reduction of H2A, H2B, H3 and H4 acetylation compared to wild-type cells in which only 5% of polytene nuclei (n=50) showed a weak staining (Figure 3A and 3D, Figure S4). Nevertheless, the overall localization of non-acetylated histones in *sea* mutants remained undistinguishable from wild-type, suggesting that acetylation, but not the loading of histones onto chromatin is affected (Figure 3C; data not shown). To confirm these results, we attempted Western blots of chromosomal protein extracts from different *sea* mutants using the same antibodies. Although the anti-pan AcH3, AcH2A and AcH2B antibodies did not recognize specific bands upon Western blotting, the anti-AcH4 yielded unambiguous results. As

expected, acetylation of H4 appeared significantly reduced (50%) in *sea* mutant extracts compared to wild-type (Figure 3D). Moreover, we verified that the reduction of H4 acetylation was specific for *sea* mutants as other mutants exhibiting chromosome aberrations, such as *tefu/atm*, maintained normal levels of acetylation (Figure 3D). To test whether the effect of Sea depletion on histone acetylation was indirect, through affecting Histone Acetyl Transferases (HATs), we assayed the activity of HATs in both wild-type and *sea* extracts. No significant difference in activity was observed (Figure S5). Collectively, these data strongly suggest that *sea* plays a fundamental role in supplying Acetyl-CoA needed for nucleosome histone acetylation. As histone tail acetylation has been recently reported as playing an essential role in the maintenance of chromatin integrity and in DNA repair (8, 9), these observations provide a potential mechanistic insight into the chromosome breakage phenotype observed in *sea* mutants.

Acetylation of histones ultimately results from a balance between levels of HAT-mediated acetylation and rates of deacetylation catalyzed by histone deacetylases (HDACs) (25). We therefore sought to determine whether the frequency of chromosome breaks observed in *sea* mutants that may reflect the decrease in global histone acetylation could be rescued by inhibition of HDACs. We observed that treatment of mutant larvae with the HDAC inhibitor trichostatin A (TSA) significantly suppressed the *sea* mutant chromosome break phenotype (Figure S6), supporting the view that *sea*-induced histone (de)acetylation leads to chromosome fragmentation.

**Inhibition of *SLC25A1* in primary human fibroblasts leads to chromosome breaks and reduced histone acetylation**

To investigate whether the above mechanism is conserved from *Drosophila* to humans, we studied the effect of *SLC25A1* inhibition on chromosome integrity. Transfection of primary human fibroblasts with siRNA duplexes against *SLC25A1* resulted in a 70% reduction of SLC25A1 protein levels (Figure 4A). Notably, 60% of siRNA-treated cells (n= 50) exhibited chromosome aberrations

following siRNA treatment while in untreated or mock-treated cells (n= 50 in both cases) breaks occurred in less than 3% (data not shown). The inhibition of *SLC25A1* induced ~ 1.3 % of chromosome aberrations per cell (n=50) while ~ 0.04% (n=50) and ~0.02% (n=50) chromosome aberrations per cell were found in untreated and mock-treated cells, respectively (Figure 4E). Interestingly, the chromosome aberrations seen in human fibroblasts consisted of both chromatid and chromosome breaks as well as chromosome exchanges (Figure 4B, C, and D), unequivocally phenocopying the *sea*-induced chromosome aberrations seen in *Drosophila*. In addition, western blots of *SLC25A1* siRNA-treated nuclear extracts showed a significant reduction (70%) of H4 acetylation with respect to untreated or mock treated fibroblasts (Figure 4F). Together, these data strongly indicate that human *SLC25A1*, as in its *Drosophila* counterpart, is important in controlling physiological histone acetylation and chromosome stability.

## Discussion

Citrate is a central metabolite for energy generation in most cells. It is produced in mitochondria and can be used either in the Krebs' cycle or released in the cytoplasm through a specific mitochondrial carrier belonging to the SLC25 gene family [20]. Here we report that dysfunction in the mitochondria citrate carrier SLC25A1 unexpectedly leads to chromosome breaks in *Drosophila* and human primary fibroblasts, strongly indicating that the correct transportation of citrate is required for genome stability. We also show that mutations in *SLC25A1* cause a global reduction of histone acetylation, indicating that, in addition to fatty acids and sterols synthesis, citrate-derived Acetyl CoA is also used for histones lysine acetylation. Much evidence has suggested that loss of histone acetylation affects DNA repair after DSB (8, 9), explaining in principle the frequent chromosome breaks observed in both *sea* mutant neuroblasts and *SLC25A1* siRNA-treated human fibroblasts.

Interestingly, *sea*-induced chromosome breakage is rescued by treating mutant cells with citrate and HDAC inhibitor trichostatin A, thus confirming a direct link between citrate deprivation, histone acetylation defects and chromosome fragmentation. However, incubation of *sea* mutant larvae with non physiological levels of acetate, the substrate used by Acetyl-CoA sinthetase (AceCS), did not lead to a reduction of chromosome breaks (data not shown), suggesting that Drosophila may not use acetate as a major source of Acetyl-CoA.

As histone acetylation can have global effects in gene transcription, it can be argued that the observed *sea* chromosome breakage could be a consequence of silencing of genes required for chromosome integrity. However, we think this is unlikely since most of the Drosophila mutations in genes involved in DNA repair so far characterized, in addition to DSBs, also cause telomeric fusions, a phenotype that we did not observe in *sea* mutants.

Recently, it has been reported that inhibition of ATP Citrate Lyase (ACL), the enzyme working just downstream from SLC25A1, significantly decreased the amount of histone acetylation (24). Wellen *et al* showed that high ACL activity is not a general requirement for cellular acetylation events, and that acetylation of histones might be specifically linked to the pool of citrate-derived acetyl-CoA produced by ACL. These findings are consistent with our observations on histone (de)acetylation defects as a consequence of poor citrate transport from mitochondria. Our results and those of Wellen *et al* together provide very strong evidence for the existance of a direct link between cellular metabolism and histone acetylation. However, our study highlights an unprecedented and evolutionary conserved role for citrate metabolism in the maintenance of genome integrity.

SLC25A1 is a fundamental factor for intermediary metabolism (20) and plays a crucial role in the regulation of glucose-stimulated insulin secretion in mammalian cells (26, 27). Furthermore,

*SLC25A1* has recently been reported as one of the six genes encoding mitochondrial proteins that map in the 1.5 Mb region and removed in DiGeorge/22q11 Deletion Syndrome (28). Alterations in citrate metabolism in mammals also have several pathophysiological consequences and can lead to cancer (i.e. prostate cancer (29)). However, how changes in citrate transport and metabolism are involved in the development of malignancy still remains unclear. The present study suggests a novel and evolutionary conserved role for Sea/SLC25A1, providing an additional level of regulation of histone acetylation and chromosome integrity. It would be of interest in the future to establish whether the novel and conserved link between citrate transport, chromatin epigenetic modifications and genome stability described above may be pivotal for the understanding of specific human genetic diseases including cancer.

## Materials and Methods

### *Drosophila* strains and crosses.

The *sea*$^{EP}$ mutation, that corresponds to *l(3)EP3364,* and the *Df(3R)Mx-1* that uncovers *sea,* were obtained from the Bloomington Stock Center. *sea*$^{\Delta 24}$ was generated by Delta 2-3-induced incomplete excision of *l(3)EP3364* inserted into the *CG6782* gene. The *mei-41(atr), mus304(atrip), tefu (atm), mre11* and *rad50* mutations have been previously described (14-18, 30, 31). *mei41*$^{29D}$ *sea* double mutants were obtained by crossing *mei41*$^{29D}$*/FM7-GFP; sea/TM6B* females to *FM7-GFP/Y, sea/TM6B* males. *tefu*$^{atm6}$ *sea* $^{\Delta 24}$ and *mus304* $^{D4}$ *sea* $^{\Delta 24}$ double mutants were generated by recombination and balanced over *TM6B. rad50*$^{\Delta 5.1}$ *sea* and *mre11 sea* were obtained by *inter se* mating of *mre11 (*or *rad50*$^{\Delta 5.1}$*)/CyO-GFP; sea /TM6B* and *mre11 (*or *rad50*$^{\Delta 5.1}$*)/CyO-GFP;cav/TM6B* flies. Larvae which were homozygous for both mutations were selected on the basis of their non *–GFP* and /or non-*Tubby* phenotypes. Detailed genetic information about the balancers used in this study is available at Flybase (http://flybase.bio.indiana.edu/). Oregon-R is a standard laboratory wild-type strain. All stocks were raised and crosses carried out at 25°C on standard Drosophila medium.

Citrate and Trichostatin A treatments were performed by feeding both mutant and control 1$^{st}$ instar larvae with a solution of 1% sucrose containing citrate (to a final concentration of 0.1M or 0.01 M) or trichostatin A (60 μM or10 μM). After 4 days, treated larvae were dissected for chromosome analysis.

### Chromosome cytology, immunostaining and microscopy.

DAPI-stained, colchicine-treated larval brain chromosome preparations for the analysis of chromosome aberration in Drosophila were made as previously described (32). Preparations for the

analysis of MI and AF were obtained in the same way, excluding both colchicine and hypotonic treatments. Chromosome preparations and fixation for immunostaining with anti histone antibodies were carried out as described previously (33). Slides were frozen in liquid nitrogen and after flipping off the coverslip, immediately immersed in cold TBS for 5 minutes in ice. Slides were then washed in TBS-T (TBS containing 0.1% Tween20 and incubated overnight with the anti-H3 (diluted 1:50), anti H4 (diluted 1:50), anti-panAcLys (1:50) anti-pan AcH2A/B (1:25), anti-panAcH3 (1:100) or anti-panAcH4 (1:300), all from Upstate/Millipore (Billerica, MA). The secondary antibody incubation was performed using CY3-conjugated donkey anti-rabbit antibody (Jackson Laboratory, West Grove, PA), diluted 1:200, for 2 hr at room temperature. Dissection and fixation of brains from third instar larvae for immunostaining with anti-Sea and anti-Skap antibodies were performed as described in Bonaccorsi et al (2000)(34). For anti-Sea/anti-Skap double staining, brain preparations were incubated overnight at 4°C with anti-Skap (1:50 in PBS). A secondary antibody incubation was performed using both the FITC-conjugated anti-mouse IgG+IgM (1:20 in PBS; Jackson laboratories) and Alexa 555-conjugated anti-Sea (1:50), for 2 h at room temperature.

To obtain polytene chromosome for anti-histone immunostaining, salivary glands from third instar larvae were dissected in 0.7% NaCl, fixed for 5 min with 2% formaldehyde in 45% acetic acid, and squashed in the same fixative. Immunostaining was performed as described above for mitotic chromosome histone staining. Mitotic and polytene chromosome preparations were analyzed using a Zeiss Axioplan epifluorescence microscope (CarlZeiss, Obezkochen, Germany), equipped with a cooled CCD camera (Photometrics, Woburn, MA). Gray-scale digital images were collected separately, converted to Photoshop format, pseudocolored, and merged.

Chromosome integrity of *SLC25A1* siRNA-treated, mock-treated and untreated human fibroblasts was evaluated as previously described (35). Briefly, colcemid (0.05 □g/ml, Gibco BRL; Gaithersburg MD) was added to the cultures for 90 min followed by a 20 min incubation in 0.075 M KCl at 37 °C and multiple changes of Carnoy's fixative (3:1

methanol: acetic acid). Fifty metaphases for each treatment were analyzed. Chromosomal aberrations were visualized by staining slides in Giemsa stain and detected by direct microscope visualization.

**Rescue construct and germline transformation**

To generate the rescue construct, a *sea*-encoding full length cDNA (LD46175, obtained from Drosophila Genomics Resource Center) was cloned into the hsC4Y plasmid (a generous gift from V. Pirrotta) under the control of a heat shock promoter. Germline transformation with the resulting construct was carried out by the BestGene Company (Chino Hills, CA) using standard procedures.

**Mitochondria and nuclear extracts**

Mitochondria were extracted from third instar larvae by differential centrifugation. A total of 500 wild type and mutant larvae were decanted into a chilled mortar and homogenized with a pestle in 2 ml of ice-cold isolating medium (250 mM sucrose, 10 mM Tris-HCl, 1 mM EDTA, 0,5% (w/v) allumine oxide, pH 7.4). All procedures were carried out at 4°C on ice**.** The homogenate was passed through two layers of absorbent muslin and immediately centrifuged at 1500 rpm for 10 min to remove debris and nuclei. The procedure was repeated with the pellet. The supernatants were pooled, passed through one layer of muslin and centrifuged at 10000 rpm for 10 min. The pellet, which contained mitochondria, was carefully resuspended and the mitochondrial fraction was stored at -80°C until use. Bradford protein estimation was carried out to equalize the protein concentration between mutant and wild-type larvae extracts. Mitochondria were then solubilized with a buffer containing 1.5% Triton X-114 (w/v), 10 mM $Na_2SO_4$ and 5 mM Pipes (pH 7.0) at a final concentration of 1 mg/ml. After incubation for 10 min at 2°C, the mixture was centrifuged at 25,000

*g* for 20 min at 2°C, and the supernatant was referred to as the mitochondrial extract. The cytosolic fraction was obtained by centrifuging the postmitochondrial supernatant at 40000 rpm for 30 min.

Protein nuclear extracts for Drosophila larvae were prepared as described in La Rocca et al. (2007) (36). ~1 μg of extract/lane was loaded for western blot analysis.

**Mitochondria reconstitution and Transport Measurements**

The mitochondria extract was reconstituted by cyclic removal of detergent (37). The reconstitution mixture consisted of protein solution (50 μL, 0.09 mg), 10% Triton X-114 (75 μL), 10% phospholipids (egg lecithin from Fluka) as sonicated liposomes (100 μL), 10 mM citrate, cardiolipin (0.6 mg; Sigma), 20 mM PIPES, pH 7.0, and water (final volume, 700 μL). The mixture was recycled 13 times through an Amberlite column. All operations were performed at 4°C, except for the passages through Amberlite, which were carried out at room temperature.

To measure the citrate transport, external substrate was removed from the proteoliposomes on Sephadex G-75 columns preequilibrated with buffer A (50 mM NaCl and 10 mM PIPES, pH 7.0). Transport at 25°C was initiated by the addition of 0.5 mM [$^{14}$C]Citrate (from Amersham) to the eluted proteoliposomes and terminated by "inhibitor-stop" method with the addition of 20 mM 1,2,3-BenzeneTricarboxylate (37). In controls, the inhibitors were added simultaneously to the labeled substrate. Finally, the external radioactivity was removed on Sephadex G-75 and radioactivity in the liposomes was measured (37). Transport activity was calculated by subtracting the control values from the experimental values.

**Antibodies and Western blotting**

To generate the anti-Sea antibody, a purified recombinant-Sea protein (21) was sent to Sigma for the generation of rabbit polyclonal antibodies. Western blotting was performed as previously

described by Somma et al. (2002); mitochondria lysates (40 µg), nuclear protein extracts (20 µg) and fibroblast lysates (40 µg) were separated by SDS-PAGE and transferred to nitrocellulose membranes. The antibody dilutions were: anti-Sea, 1:2000; anti H3 and anti H4, 1: 4000; anti AcH3and anti AcH4, 1: 8000; anti-porine, 1:500; anti-C terminal-SLC25A1 1:2500 (38).

To obtain a fluorescently labelled Anti-Sea antibody, purified anti-Sea was dialyzed into phosphate-buffered saline (PBS) (Slide-A-Lyzer Dialysis Cassettes 3.5K MWCO, Pierce, Rockford, IL, USA) and concentrated to 2 mg/mL using a Centrifugal Filter and Tube (Millipore, Bedford, MA). ~1mg of anti-Sea antibody was then conjugated to Alexa Fluor-555 (Molecular Probes). according to the protocol supplied by the manufacturer (Molecular Probes). The unreacted dye was removed using 0,5 ml Zeba Desalt Spin Columns (Pierce, Rockford, IL, USA).

**Measurement of Citrate by Gas Chromatography/Mass Spectrometry**

Citric acid amounts from either mitochondria or cytosolic fraction were measured using a modified gas chromatography/mass spectrometry (GC/MS)-based method. In particular, three aliquots of the mitochondrial or cytosolic fraction of the cells were treated with 300 µl of 0.1 M HCl each and added with 0, 10 and 20 µl of a100 ppm standard solution of citric acid. pH of the extract was adjusted to 8 –9 with KOH. Ethoxyamine (Sigma) was added, and the mixture was incubated at room temperature for 30 min. Next, pH was adjusted to 1–2 with HCl, 50 mg of NaCl were added, and samples vortexed and extracted twice with ethyl acetate (VWR). Upper phases containing the organic acid were combined and subsequently dried under nitrogen. 8 µl of pyridine and 100 µl of N,O-Bis(trimethylsilyl)trifluoroacetamide were added, and the samples were incubated at 90 °C for 30 min. The citric acid derivative was separated and determined on a 6890N gas-chromatograph (Agilent, Palo Alto, CA, USA) equipped with an 7683B autosampler (Agilent), a split/splitless injection port and a quadrupole mass spectrometer detector mod. 5973 inert (Agilent), electron impact 70 eV, ion source temperature 280°C, interface temperature 280°C. The injection volume

was 2 µL in splitless mode. The chromatographic separation was performed on a chemically bonded fused silica capillary column DB-35MS (Agilent), 0.25 mm internal diameter, 0.25 µm film thickness, 30 m length, connected to a 2 m long deactivated fused silica capillary pre-column. GC conditions: initial temperature 80 °C, 2 min isothermal, 6 °C/min up to 220 °C, 10 °C/min up to 300 °C. Carrier gas: He, constant flow 1.2 ml/min. The trimethylsilyl derivatives were quantified by selected ion monitoring (*m/z* 465) using the standard addition method.

**Cell culture**

Normal primary human fibroblasts, previously described (39), were grown in Dulbecco's minimal essential medium (DMEM, Gibco BRL; Gaithersburg MD) supplemented with 10% fetal calf serum and antibiotics in a humidified 5% $CO_2$ atmosphere.

**siRNA synthesis and cell treatment**

siRNA corresponding to *SLC25A1* mRNA was designed with two base overhangs. The following gene-specific sequence (Qiagen, Netherlands) was used: siRNA - *SLC25A1* 5'-CAG GGC CTG GAG GCG CAC A dTT-3', Scrambled RNA, *SLC25A1* 5'- GCT ACG GAC AGC CGG CAG G dTT-3', was constructed as control. Cells (at 40-60% confluence) were transfected with 10 nM siRNA by using Interferin (Celbio, Italy).

**RNA isolation and Semiquantitative RT-PCR.**

Total RNA was isolated from wild-type (Oregon R) and mutant larvae using the RNeasy Mini Kit (Qiagen). 50 ng of RNA were reverse transcribed and amplified using Access RT-PCR System kit (Promega). The *rp49* gene was used as an internal control. The forward and reverse gene-specific primers, were as follows: *sea*, forward 5' CTGTCCCCATCGCCACTTCA 3', reverse *5'*

CTATAGCCACTTACCCATTGC 3'; *rp49*, forward 5′ ATCGGTTACGGATCGAACAA 3′ and *rp49* reverse 5′ GACAATCTCCTTGCGCTTCT 3′. The PCR products were analysed by 1% agarose gel electrophoresis. Band intensities were quantified using Quantity One 1-D Analysis Software (Biorad, Hercules, CA).

**Acknowledgments**

We are very grateful to Yikang Rong for allowing P. M. to perform some of the work described here in his laboratory. The anti-Porin and anti-Skap antibodies were kindly provided by Vito De Pinto and James Wakefield, respectively. We thank Yikang Rong, Maurizio Gatti and Vincenza Dolce for helpful discussion, Giuseppe Vecchio and Giuseppina De Filippis for technical assistance and James Wakefield for a critical reading of the manuscript.

**Funding**

This work is partially funded by grants from Istituto Toscano Tumori, Consiglio Nazionale delle Ricerche (CNR, RSTL), Fondazione Cassa di Risparmio delle Province Lombarde (CARIPLO) to A.M., by grants from Fondazione Telethon, Giovanni Armenise Harvard Foundation, MIUR (Italian Ministry of University and Research), HFSP, Compagnia San Paolo and AIRC (Italian Association for Cancer Research) to D.F.V.C . G.B. was supported by an AIRC fellowship.

This paper is dedicated to the memory of our University of L'Aquila students Nicola Bianchi and Giusy Antonini whose dreams of being scientists were dramatically shattered by the 6th April '09 earthquake.

**References**

1. McKinnon, P.J. and Caldecott, K.W. (2007) DNA strand break repair and human genetic disease. *Annu Rev Genomics Hum Genet*, **8**, 37-55.
2. Coleman, W.B. and Tsongalis, G.J. (2006) Molecular mechanisms of human carcinogenesis. *Exs*, 321-349.

3. Gasparini, P., Sozzi, G. and Pierotti, M.A. (2007) The role of chromosomal alterations in human cancer development. *J Cell Biochem,* **102**, 320-331.
4. Hanahan, D. and Weinberg, R.A. (2000) The hallmarks of cancer. *Cell,* **100**, 57-70.
5. Bailey, S.M. and Bedford, J.S. (2006) Studies on chromosome aberration induction: what can they tell us about DNA repair? *DNA Repair (Amst),* **5**, 1171-1181.
6. Longhese, M.P., Mantiero, D. and Clerici, M. (2006) The cellular response to chromosome breakage. *Mol Microbiol,* **60**, 1099-1108.
7. Wyman, C. and Kanaar, R. (2006) DNA double-strand break repair: all's well that ends well. *Annu Rev Genet,* **40**, 363-383.
8. van Attikum, H. and Gasser, S.M. (2005) The histone code at DNA breaks: a guide to repair? *Nat Rev Mol Cell Biol,* **6**, 757-765.
9. Groth, A., Rocha, W., Verreault, A. and Almouzni, G. (2007) Chromatin challenges during DNA replication and repair. *Cell,* **128**, 721-733.
10. Celeste, A., Difilippantonio, S., Difilippantonio, M.J., Fernandez-Capetillo, O., Pilch, D.R., Sedelnikova, O.A., Eckhaus, M., Ried, T., Bonner, W.M. and Nussenzweig, A. (2003) H2AX haploinsufficiency modifies genomic stability and tumor susceptibility. *Cell,* **114**, 371-383.
11. Lou, Z., Minter-Dykhouse, K., Franco, S., Gostissa, M., Rivera, M.A., Celeste, A., Manis, J.P., van Deursen, J., Nussenzweig, A., Paull, T.T. *et al.* (2006) MDC1 maintains genomic stability by participating in the amplification of ATM-dependent DNA damage signals. *Mol Cell,* **21**, 187-200.
12. Kouzarides, T. (2007) Chromatin modifications and their function. *Cell,* 128, 693-705.
13. Millar, C.B. and Grunstein, M. (2006) Genome-wide patterns of histone modifications in yeast. *Nat Rev Mol Cell Biol,* **7**, 657-666.
14. Hari, K.L., Santerre, A., Sekelsky, J.J., McKim, K.S., Boyd, J.B. and Hawley, R.S. (1995) The mei-41 gene of D. melanogaster is a structural and functional homolog of the human ataxia telangiectasia gene. *Cell,* **82**, 815-821.
15. Brodsky, M.H., Sekelsky, J.J., Tsang, G., Hawley, R.S. and Rubin, G.M. (2000) mus304 encodes a novel DNA damage checkpoint protein required during Drosophila development. *Genes Dev,* **14**, 666-678.
16. Ciapponi, L., Cenci, G., Ducau, J., Flores, C., Johnson-Schlitz, D., Gorski, M.M., Engels, W.R. and Gatti, M. (2004) The Drosophila Mre11/Rad50 complex is required to prevent both telomeric fusion and chromosome breakage. *Curr Biol,* **14**, 1360-1366.
17. Bi, X., Wei, S.C. and Rong, Y.S. (2004) Telomere protection without a telomerase; the role of ATM and Mre11 in Drosophila telomere maintenance. *Curr Biol,* **14**, 1348-1353.
18. Oikemus, S.R., McGinnis, N., Queiroz-Machado, J., Tukachinsky, H., Takada, S., Sunkel, C.E. and Brodsky, M.H. (2004) Drosophila atm/telomere fusion is required for telomeric localization of HP1 and telomere position effect. *Genes Dev,* **18**, 1850-1861.
19. Silva, E., Tiong, S., Pedersen, M., Homola, E., Royou, A., Fasulo, B., Siriaco, G. and Campbell, S.D. (2004) ATM is required for telomere maintenance and chromosome stability during Drosophila development. *Curr Biol,* **14**, 1341-1347.
20. Palmieri, F. (2004) The mitochondrial transporter family (SLC25): physiological and pathological implications. *Pflugers Arch,* **447**, 689-709.
21. Carrisi, C., Madeo, M., Morciano, P., Dolce, V., Cenci, G., Cappello, A.R., Mazzeo, G., Iacopetta, D. and Capobianco, L. (2008) Identification of the Drosophila melanogaster mitochondrial citrate carrier: bacterial expression, reconstitution, functional characterization and developmental distribution. *J Biochem,* **144**, 389-392.
22. Hughes, J.R., Meireles, A.M., Fisher, K.H., Garcia, A., Antrobus, P.R., Wainman, A., Zitzmann, N., Deane, C., Ohkura, H. and Wakefield, J.G. (2008) A microtubule interactome: complexes with roles in cell cycle and mitosis. *PLoS Biol,* **6**, e98.

23. Owusu-Ansah, E., Yavari, A., Mandal, S. and Banerjee, U. (2008) Distinct mitochondrial retrograde signals control the G1-S cell cycle checkpoint. *Nat Genet,* **40**, 356-361.
24. Wellen, K.E., Hatzivassiliou, G., Sachdeva, U.M., Bui, T.V., Cross, J.R. and Thompson, C.B. (2009) ATP-citrate lyase links cellular metabolism to histone acetylation. *Science,* **324**, 1076-1080.
25. Kurdistani, S.K. and Grunstein, M. (2003) Histone acetylation and deacetylation in yeast. *Nat Rev Mol Cell Biol,* **4**, 276-284.
26. Joseph, J.W., Jensen, M.V., Ilkayeva, O., Palmieri, F., Alarcon, C., Rhodes, C.J. and Newgard, C.B. (2006) The mitochondrial citrate/isocitrate carrier plays a regulatory role in glucose-stimulated insulin secretion. *J Biol Chem,* **281**, 35624-35632.
27. Ronnebaum, S.M., Ilkayeva, O., Burgess, S.C., Joseph, J.W., Lu, D., Stevens, R.D., Becker, T.C., Sherry, A.D., Newgard, C.B. and Jensen, M.V. (2006) A pyruvate cycling pathway involving cytosolic NADP-dependent isocitrate dehydrogenase regulates glucose-stimulated insulin secretion. *J Biol Chem,* **281**, 30593-30602.
28. Maynard, T.M., Meechan, D.W., Dudevoir, M.L., Gopalakrishna, D., Peters, A.Z., Heindel, C.C., Sugimoto, T.J., Wu, Y., Lieberman, J.A. and Lamantia, A.S. (2008) Mitochondrial localization and function of a subset of 22q11 deletion syndrome candidate genes. *Mol Cell Neurosci,* **39**, 439-51.
29. Mycielska, M.E., Patel, A., Rizaner, N., Mazurek, M.P., Keun, H., Patel, A., Ganapathy, V. and Djamgoz, M.B. (2009) Citrate transport and metabolism in mammalian cells: prostate epithelial cells and prostate cancer. *Bioessays,* **31**, 10-20.
30. Ciapponi, L., Cenci, G. and Gatti, M. (2006) The Drosophila Nbs protein functions in multiple pathways for the maintenance of genome stability. *Genetics,* **173**, 1447-54.
31. Oikemus, S.R., Queiroz-Machado, J., Lai, K., McGinnis, N., Sunkel, C. and Brodsky, M.H. (2006) Epigenetic telomere protection by Drosophila DNA damage response pathways. *PLoS Genet,* **2**, e71.
32. Cenci, G., Rawson, R.B., Belloni, G., Castrillon, D.H., Tudor, M., Petrucci, R., Goldberg, M.L., Wasserman, S.A. and Gatti, M. (1997) UbcD1, a Drosophila ubiquitin-conjugating enzyme required for proper telomere behavior. *Genes Dev,* **11**, 863-875.
33. Cenci, G., Siriaco, G., Raffa, G.D., Kellum, R. and Gatti, M. (2003) The Drosophila HOAP protein is required for telomere capping. *Nat Cell Biol,* **5**, 82-84.
34. Bonaccorsi, S., Giansanti, M.G. and Gatti, M. (2000) Spindle assembly in Drosophila neuroblasts and ganglion mother cells. *Nat Cell Biol,* **2**, 54-56.
35. Revenkova, E., Focarelli, M.L., Susani, L., Paulis, M., Bassi, M.T., Mannini, L., Frattini, A., Delia, D., Krantz, I., Vezzoni, P. *et al.* (2008) Cornelia De Lange Syndrome mutations in Smc1a or Smc3 affect binding to Dna. *Hum Mol Genet*, **18**, 418-427
36. La Rocca, G., Burgio, G. and Corona, D.F. (2007) A protein nuclear extract from D. melanogaster larval tissues. *Fly (Austin),* **1**, 343-345.
37. Palmieri, F., Indiveri, C., Bisaccia, F. and Iacobazzi, V. (1995) Mitochondrial metabolite carrier proteins: purification, reconstitution, and transport studies. *Methods Enzymol,* **260**, 349-369.
38. Capobianco, L., Bisaccia, F., Michel, A., Sluse, F.E. and Palmieri, F. (1995) The N- and C-termini of the tricarboxylate carrier are exposed to the cytoplasmic side of the inner mitochondrial membrane. *FEBS Lett,* **357**, 297-300.
39. Musio, A., Montagna, C., Zambroni, D., Indino, E., Barbieri, O., Citti, L., Villa, A., Ried, T. and Vezzoni, P. (2003) Inhibition of BUB1 results in genomic instability and anchorage-independent growth of normal human fibroblasts. *Cancer Res,* **63**, 2855-2863.

**Legends to Figures.**

**Figure 1. Chromosome aberrations in *sea* mutants.** DAPI-stained metaphases from wild-type (A) and *sea* mutant (B-F) larval brains. A) wild-type female metaphase. The four pairs of chromosomes are indicated by numbers and letters. B) Mutant female metaphase showing a chromosome break (thick arrow) at the pericentric region of chromosome 3. C) a female metaphase with a chromosome break (thick arrow) on chromosome 3 and a chromatid break (thin arrow) on the X. D) A mutant female metaphase showing an asymmetrical interchange (dicentric, asterisk) accompained by acentric fragments (thick arrow). E) Mutant female metaphase with a three-armed configuration (triradial, asterisk) between two chromosomes 3 associated with an acentric fragment (thin arrow). F) Mutant metaphase exhibiting extensive chromosome breaks with splinters of chromatin. G) Frequencies of chromosome aberrations observed in *sea* mutants. For each genotype a minimum of 100 cells from at least three brains were analyzed. The frequency of chromosome breaks (black bars) does not include highly fragmented nuclei with chromatin "splinters". In contrast, these cells were counted for the frequency of irregular cells (gray bars). Note that the frequency of chromosome aberrations observed in $sea^{EP}$ homozygotes is almost identical to that found in $sea^{EP}/Df$ combination, indicating that $sea^{EP}$ is a genetically null allele H) Mitotic parameters in *sea* mutants. While the MI (black bars) observed in *sea* is significantly lower than that found in wild-type (OR/R) cells, the AF (gray bars) does not change. The low MI associated with *sea* mutations is rescued by mutations in DDR genes *mei-4 (atm)* and *mus304(atrip)*, but not by mutations in *rad50* and *mre11*. *Df, Df(3R)Mx-1*.

**Figure 2**. **Functional analysis of Sea**. A) Western blot of mitochondrial extracts from wild-type and *sea* third instar larvae. The affinity-purified anti-Sea antibody specifically recognizes a band of

~33 KDa in mitochondria extracts. Sea levels are significantly reduced in *sea* mutants. Anti-Porin A was used as loading control. B) Sea localizes in discrete spots (red) in the cytoplasm of interphase mitotic cells. C) Sea localization is reduced in the cytoplasm of *sea* mutant mitotic cells. D) Punctuate localization (green) of Skap, a resident protein of the inner mitochondrial membrane, in the same cells as in B. E) Sea and Skap colocalize (yellow) indicating that Sea decorates mitochondria. F) Differences in [$^{14}$C]citrate/citrate exchange between wild type and *sea* mutant mitochondria**.** Proteoliposomes were reconstituted with the mitochondrial proteins from either wild-type (*green*) or *sea* mutant (*purple).* The data represent means of four independent experiments. G) GS/MS-based quantification of citrate levels from either cytosol or mitochondria of wild-type (green) and *sea* mutant (purple). Note the reduction of citrate in the cytosol (but not in mitochondria) of *sea* mutants with respect to wild-type. H) Suppression of chromosome breaks by supplementation with citrate. Columns indicate the frequency (%) of chromosome breaks in mutant (blue) and control (green) mitotic cells upon supplementation with 1% sucrose containing different concentrations of citrate. Statistically significant differences are indicated by "*" (*t* test; $p<0.001$). 200 cells for mutants and controls were analyzed. Error bars refer to SD.

**Figure 3. Mutations in *sea* affect histone acetylation**. (A, C) Localization pattern of acetylated-Lys (AcLys) (A) and -H4 (AcH4) (C, bottom) in wild-type and *sea* polytene chromosomes. Both Ac-Lys and Ac-H4 stainings are reduced in the mutant compared to wild-type while the localization pattern of H4 is undistinguishable from wild-type (C, top). B) Immunoblotting of chromosome extracts with anti-AcLys showing a decrease in the acetylation levels of low-molecular-weight bands (asterisk) in mutants that are likely to correspond to histones. D) Western blotting on chromosome protein extracts from wild-type and *sea* mutant third instar larvae with anti-AcH4. Reduction in the histones acetylation does not occur in wild-type (OR) or in extracts from the *tefu(atm)* mutant which exhibits chromosome breaks (and telomeric fusions).

**Figure 4. Effects of *SLC25A1* inhibition by siRNA in primary human fibroblasts**. (A) siRNA against *SLC25A1* led to a down regulation (70%) of SLC25A1 levels (lane 3) compared with untreated cells (lane 1) and mock-treated cells (lane 2). Partial metaphases showing siRNA-*SLC25A1* induced chromosome aberrations: gap (B), break (C) and dicentric (D). (e) Sixty-two chromosome aberrations occurred in 50 siRNA-treated cells while only 2 and 1 chromosome aberrations in un- and mock-treated cells (n=50). (F) Western blotting showing down regulation (70%) of the histone H4 acetylation following siRNA-*SLC25A1* treatment (lane 3), compared to untreated cells (lane 1) and mock-treated cells (lane 2). Actin was used as loading control.

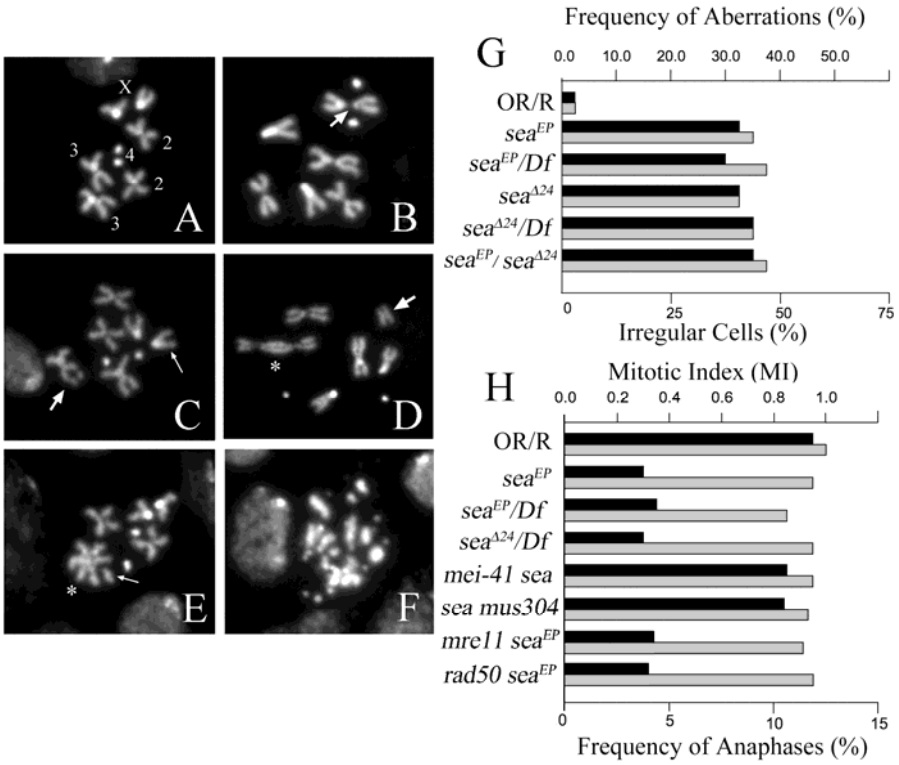


Morciano et al., Figure 1

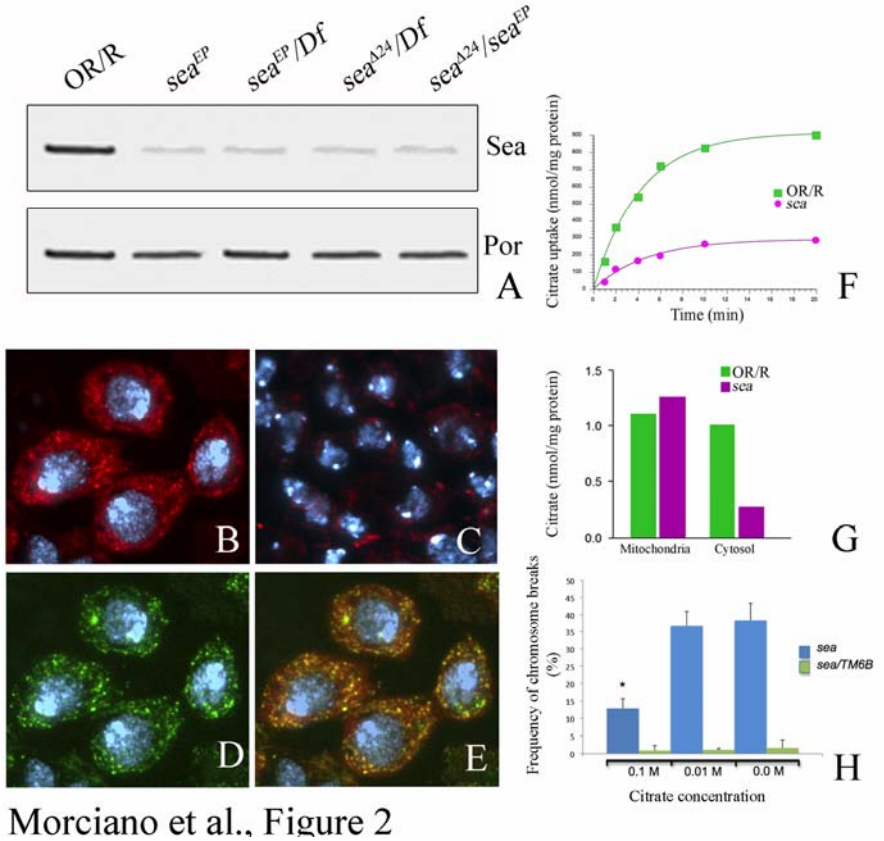


Morciano et al., Figure 2

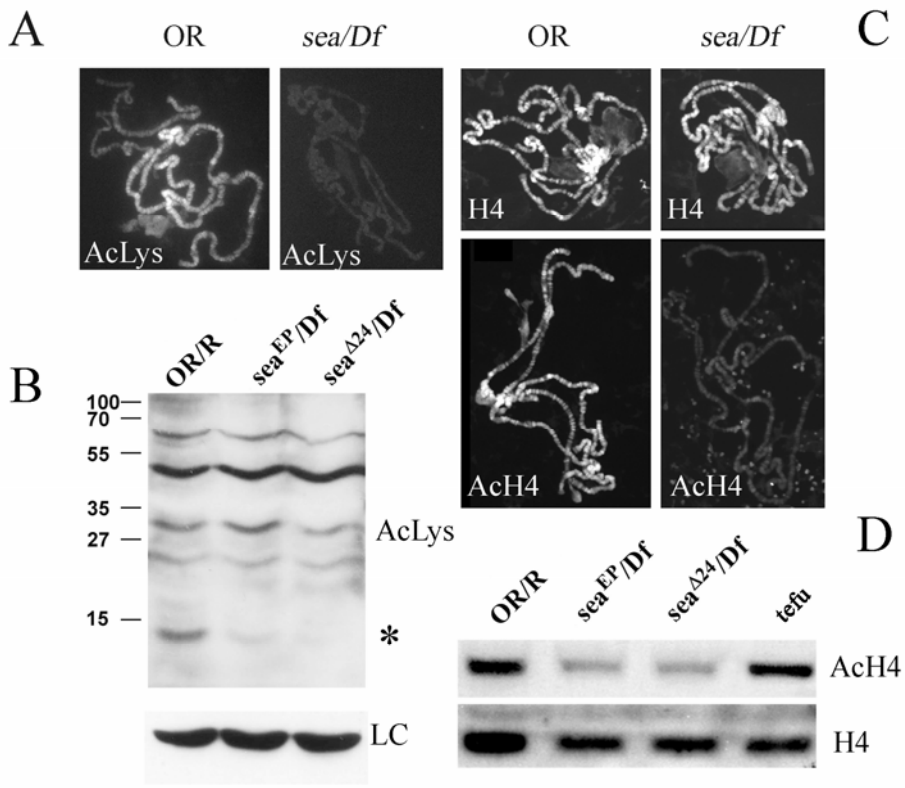


Morciano et al, Figure 3

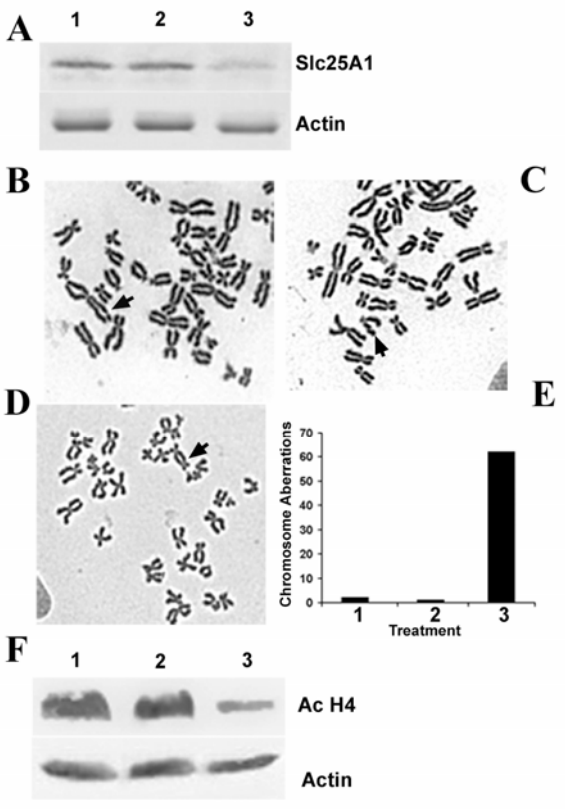


Morciano et al, Figure 4

**Abbreviations:**

Sea= Scheggia
SLC25A1= Solute carrier 25 A1
ATM= ataxia telangiectasia mutated
ATR= ATM- and Rad3-related
MI= Mitotic Index
AF= Anaphase Frequency
DDR= DNA Damage Response
Mei-41= meiotic-41
Mus304= mutagen sensitive 304
ATRIP= ATR Interacting Protein
Skap= SkpA Associated Protein
Mre11= meiotic recombination 11 protein
Tefu= Telomeric fusion
Km= Michaelis-Menten constant
Vmax= Maximum velocity
GC/MS= Gas Chromatography/Mass Spectrometry
ROS= Reactive Oxygene Species
HAT= Histone Acetyl Transferase
HDAC= Histone Deacetylase
TSA= Trichostatin A
siRNA= short interfering RNA
DSB= Double Strand Break
AceCS= Acetyl-CoA sinthetase
ACL= ATP Citrate Lyase
CNR = Consiglio Nazionale delle Ricerche
RSTL= Ricerca Spontanea a Tema Libero
MIUR= Ministero Italiano Università e Ricerca
HFSP= Human Frontier Science Program
AIRC = Associazione Italiana Ricerca sul Cancro
FM7= First Multiple
TM6= Third Multiple
GFP= Green Fluorescent Protein
CyO= Curly of Oster
TBS= Tris-Buffered Saline
PBS= Phospate-Buffered Saline
CY3= Cyanine3
CCD= Cooled-Coupled Device
DMEM= Dulbecco minimal essential medium